CHAPTER IV

RESULTS AND DISCUSSION

1. Solubility of minoxidil

The saturation solubility of MN in tri-distilled water was experimentally determined at ambient temperature. The daytime temperature monitored during the period of study was around 24-25 °C. The complete solubility data are shown in Table 4. A concentration of MN at below 90% of its saturation solubility in water (2.2 mg/ml) was used in all subsequent studies to avoid supersaturation and recrystallization of the drug due to fluctuation in ambient temperature.

Table 4. Solubility data of MN in water

Time (day)	Solubility of MN (mg/ml)			Mean (mg/ml)	SD
	1	2	3		
2	2.63	2.61	2.59	2.61	0.02
4	2.60	2.61	2.60	2.61	0.01

2. Characterization of MN niosomes

2.1 Determination of MN entrapment efficiency

MN niosomes were prepared from the compositions listed in Table 5. At least three batches were prepared to ensure feasibility of niosome formation for these formulations. It is essential to prepare niosomes at a temperature above phase-transition temperature of the non-ionic surfactant. Among all the non-ionic surfactants used in this study, Span® 60 has the highest phase transition temperature of about 50 °C (Yoshioka,

Sternberg, and Florence, 1994). Therefore, all preparations were successfully prepared at 70 °C.

Table 5. Compositions of niosome formulations studied

Non-ionic surfactant		Cholesterol (mg)	Solulan® C24 (mg)
Type	Weight (mg)		
Span® 40	67.5	27.5	5
Span® 60	57.5	37.5	5
Brij® 52	67.5	27.5	5
Brij® 76	47.5	47.5	5

MN associated with niosomal pellets and unentrapped MN in the supernatant were analyzed after separation by ultracentrifugation. Table 6 shows the amounts of unentrapped and entrapped MN in niosomal suspension, entrapment efficiency, percent MN entrapment, and total recovery of the four formulations.

Table 6. The amounts of unentrapped and entrapped MN in niosomal suspensions, entrapment efficiency, % entrapment, and total recovery of MN in MN niosomes. Data are presented as mean ± SD, n = 3.

Main component	Amount of MN*		Entrapment efficiency (μg/mg lipid)	% Entrapment	Total recovery
	Unentrapped MN (mg)	Entrapped MN (mg)			
Span® 40	11.32 ± 0.65	1.91 ± 0.03	19.13 ± 0.26	86.94 ± 1.18	100.42 ± 0.67
Span® 60	11.16 ± 0.20	2.10 ± 0.01	20.97 ± 0.05	95.32 ± 0.25	100.47 ± 1.53
Brij® 52	11.94 ± 0.07	1.43 ± 0.01	14.31 ± 0.12	65.06 ± 0.53	101.44±0.58
Brij® 76	11.50 ± 0.25	1.70 ± 0.03	17.03 ± 0.35	77.43 ± 1.58	100.22±1.64

*Total MN before separation = 13.18 mg

Entrapment efficiencies of the four MN niosomal suspensions are statistically different ($p < 0.05$) by ANOVA with Tukey's HSD test. Entrapment efficiency of the formulation with Span® 60 was higher than that of the formulation with Span® 40. This could be attributed to the structure of surfactant. Span® 40 and Span® 60 have the same head group and different alkyl chains. Span® 60 has long saturated alkyl chain and usually shows the higher entrapment than that of formulations with shorter alkyl chains (Hao et al., 2002). These results are in good agreement with the observations by Uchegbu and Florence (1995) on doxorubicin-loaded niosomes. In another previous study, sorbitan monostearate (C18) vesicles always showed increased encapsulation efficiency with respect to sorbitan monopalmitate (C16) niosomes (Manconi et al., 2002). Uchegbu and Duncan (1997) studied niosomes containing N-(2-hydroxypropyl) methacrylamide copolymer-doxorubicin. They found that the surfactants with longer alkyl chain gave vesicles with higher entrapment and vesicle size. These reports support the hypothesis that percentage of entrapment may be correlated to the higher hydrophobicity of the alkyl chain of the sorbitan esters. This is because larger vesicles are formed when the hydrophilic portion of the molecule is decreased relative to the hydrophobic portion, leading to increased entrapment. The increase in entrapment across a homologous series of Span® surfactants has been reported previously (Uchegbu and Florence, 1995). Similarly, in the Brij® series in this present study, niosomes prepared from Brij® 76 also gave higher entrapment efficiency than that of niosomes from Brij® 52 due to the difference in the length of the alkyl chains. Another research group reported similar results where the entrapment efficiency of vesicles obtained from Brij® 72 was higher than that of vesicles from Brij® 52 (Manosroi, 2003). The results of this experiment indicate that the entrapment efficiency of MN in niosomes was related to vesicle composition.

2.2 Optical microscopy

All batches of MN niosomes were viewed under an optical microscope to observe the shape of vesicles and the overall nature of the preparation. Not only did the spherical shape form, but also the tubular shape was found in the preparation. The vesicles

appearing under the light microscope varied in size. There was no detectable change in vesicle formation and its shape of all preparations after three months of storage when inspected under an optical microscope. In all preparations, no drug crystal was found over the period of three months. Figures 11-14 show optical microscopic images of MN vesicles prepared with Span® 40:Cholesterol:Solulan® C24, Span® 60:Cholesterol: Solulan® C24, Brij® 52:Cholesterol:Solulan® C24, and Brij® 76:Cholesterol:Solulan® C24, respectively.

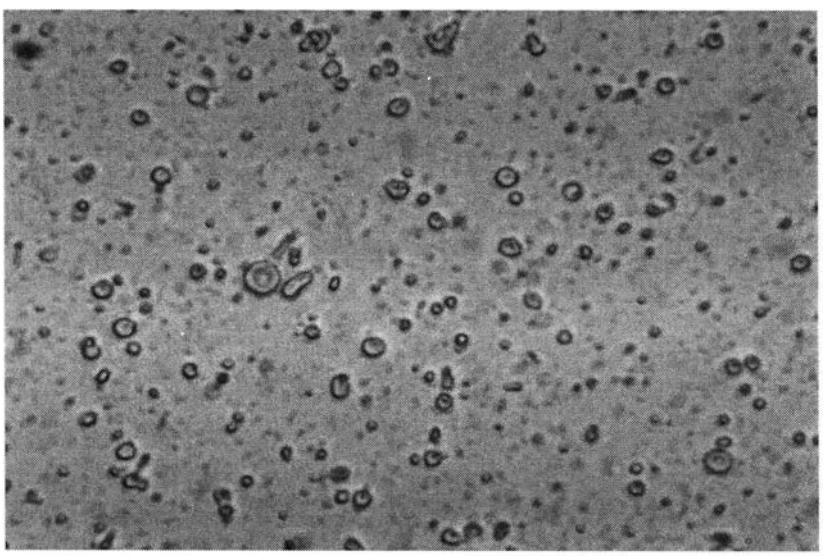

(a)

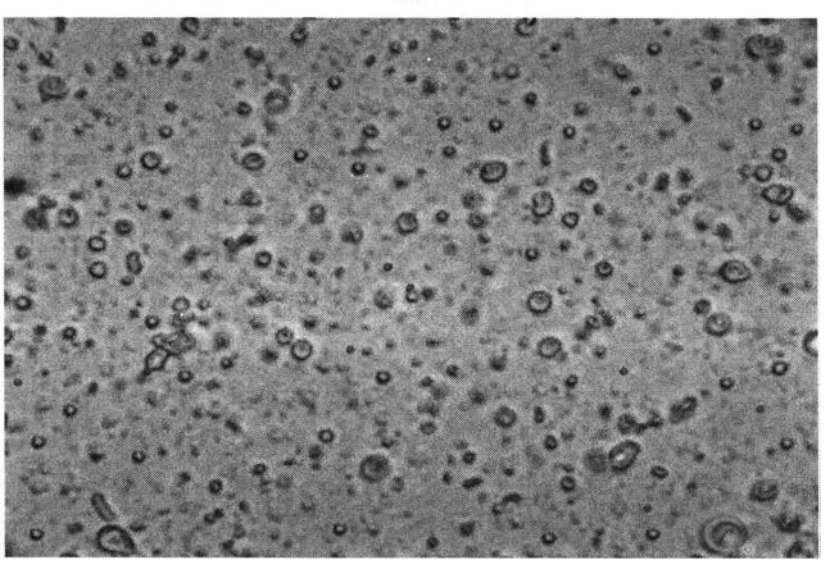

(b)

Figure 11. Photographs of Span® 40:Cholesterol:Solulan® C24 niosomes at (a) 0 month and (b) 3 months

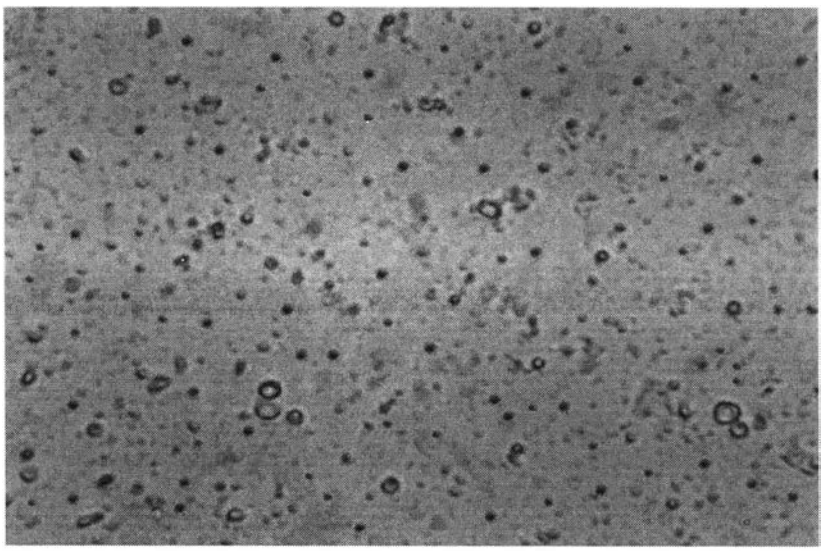

(a)

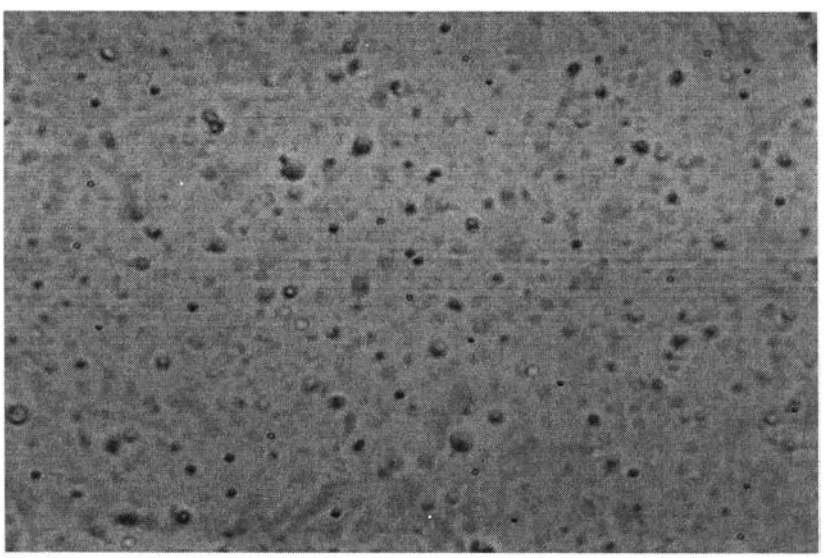

(b)

Figure 12. Photographs of Span® 60:Cholesterol:Solulan® C24 niosomes at (a) 0 month and (b) 3 months

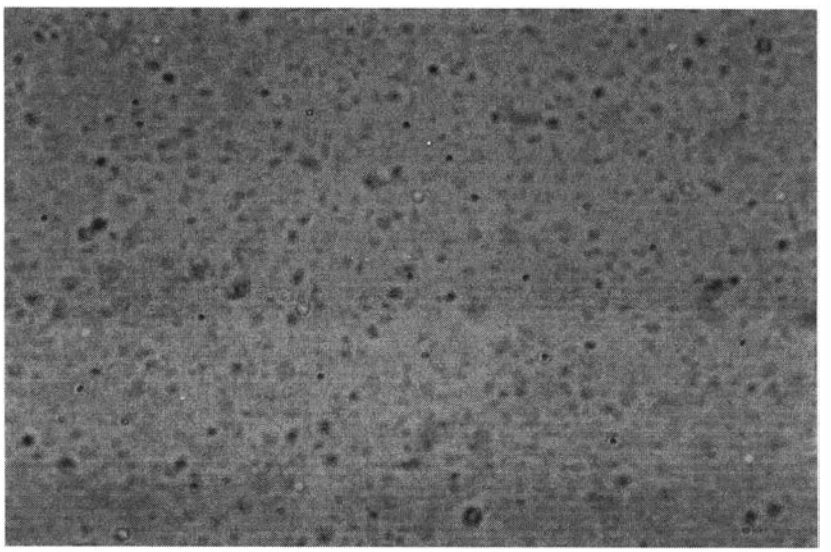

(a)

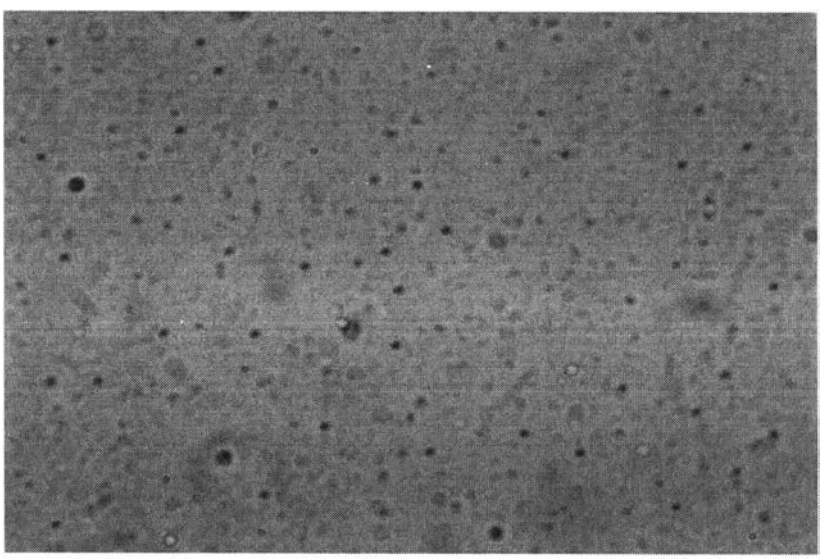

(b)

Figure 13. Photographs of Brij® 52:Cholesterol:Solulan® C24 niosomes at (a) 0 month and (b) 3 months

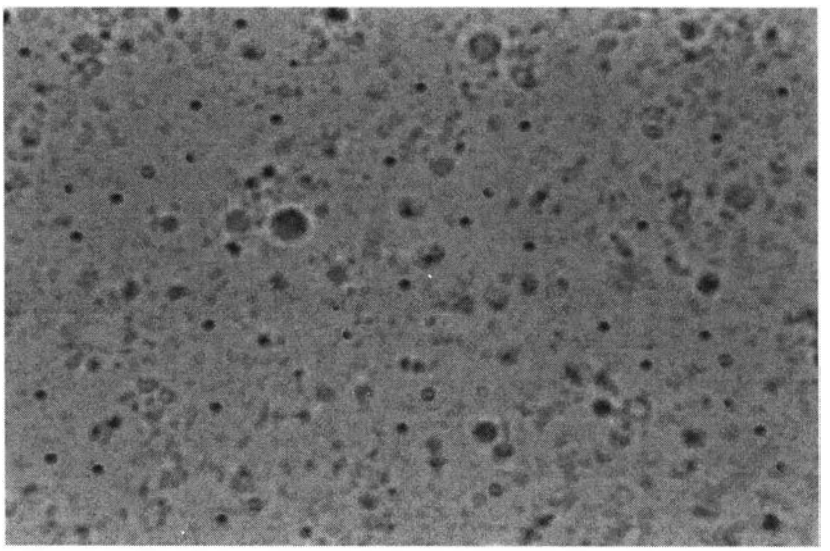

(a)

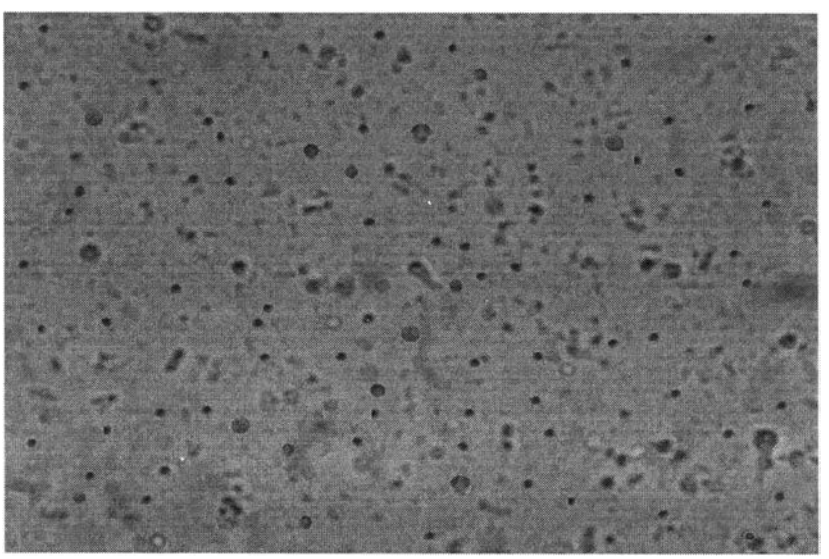

(b)

Figure 14. Photographs of Brij® 76:Cholesterol:Solulan® C24 niosomes (a) 0 month and (b) 3 months

Size analysis using laser scattering also showed multimodal distributions of these niosomes (Figure 15). The complicated size distributions made size comparison by this method inappropriate. Thus, size distribution was not used to monitor physical stability of these preparations.

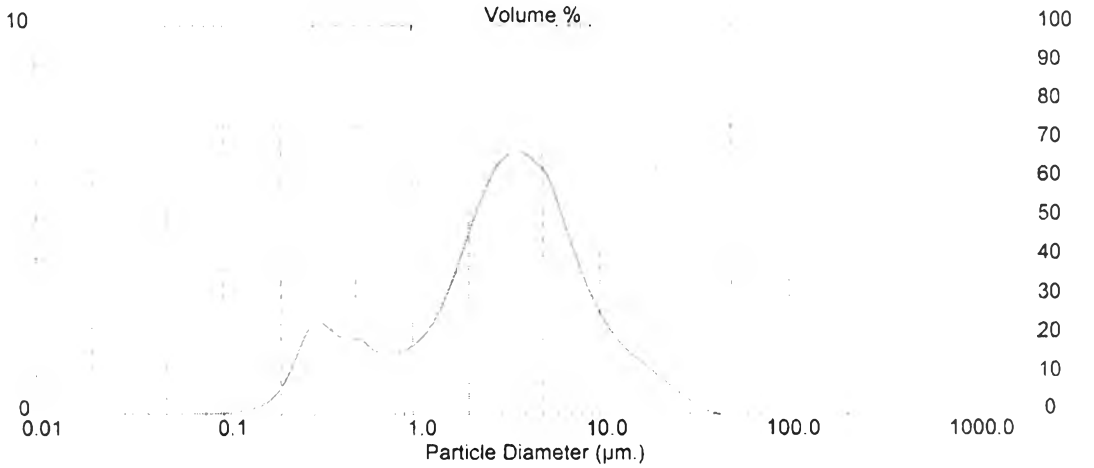

Figure 15. A representation of multimodal distributions of MN niosomes prepared from Brij® 52 (1 day after preparation)

2.3 Polarized light microscopy

Figure 16 shows polarized-light microscopic images of vesicles from Span® 40, Span® 60, Brij® 52, and Brij® 76. The sizes of vesicles composed of Brij® surfactant were smaller than the size of vesicles composed of Span® surfactant. Thus, the corresponding cross-polarized images of vesicles from Brij® surfactant (Figure 14, c and d) do not show the interference patterns as clearly as the vesicles from Span®. These interference patterns are called "Maltese cross" and are typical for lamellar structures. They have been used to identify niosomal structures as well as other closed bilayers (Manosroi et al., 2003; Maki et al., 2003; Yamashita, 2004). The Maltese crosses have various kinds of shapes, which can be divided into three types. The first one is round in shape, with four symmetry equal and broad bright double-refraction areas, and the middle part is a narrow, dark cross. The second one is irregularly round in shape with four symmetry bright double-refraction areas that are not equal to each other. The narrow dark cross in the middle is lean towards different directions. The third one is oval with four narrow bright double-refraction areas, and there is a bigger dark cross in the middle (Yang et al., 2000). Brightness or darkness of Maltese cross is changed regularly when the stage is rotated, which changes once for

each 45° turning. If there is a turning of 360°, four times of brightness and darkness appears, i.e., four extinction and four interference color phenomena occur.

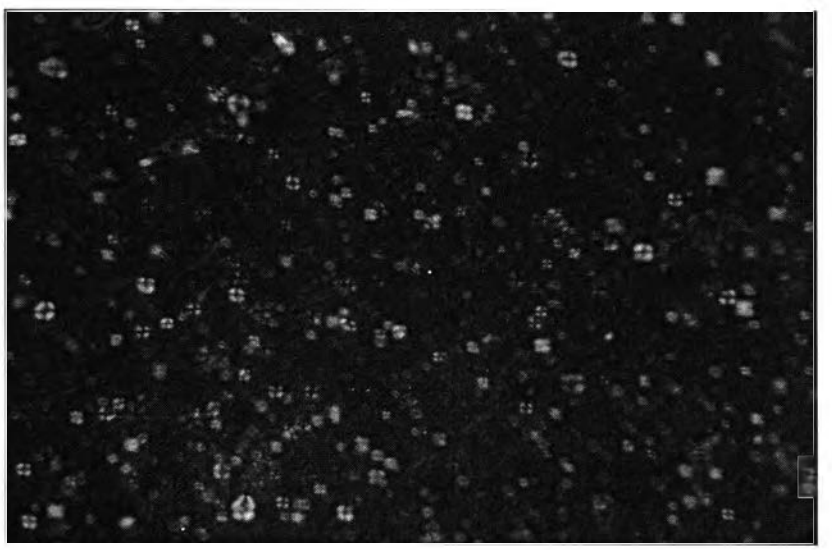

(a)

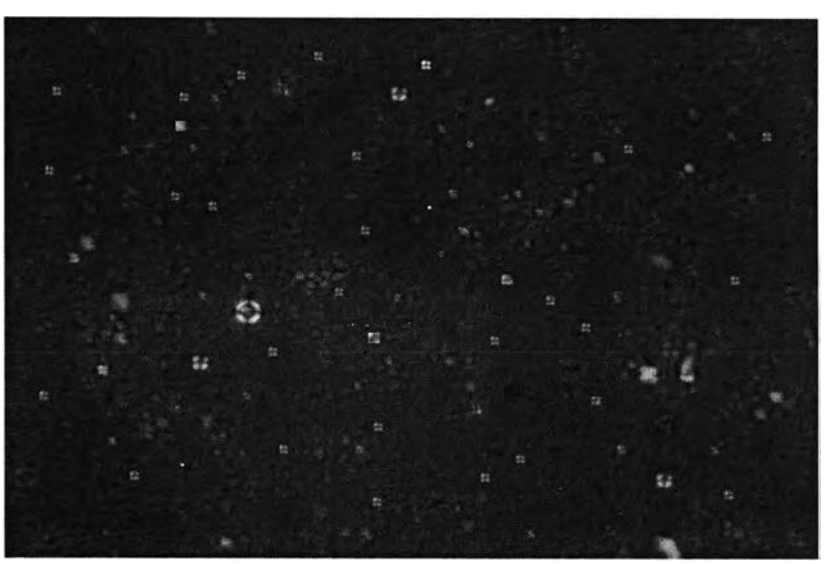

(b)

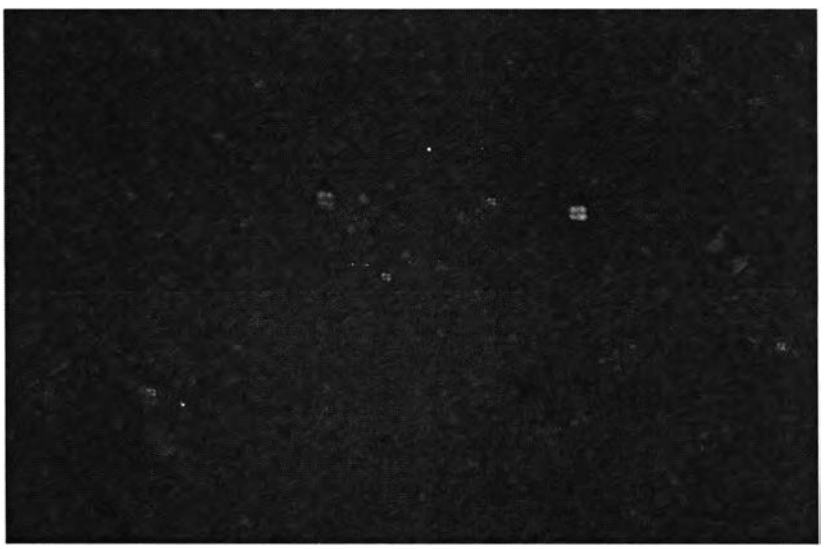

(c)

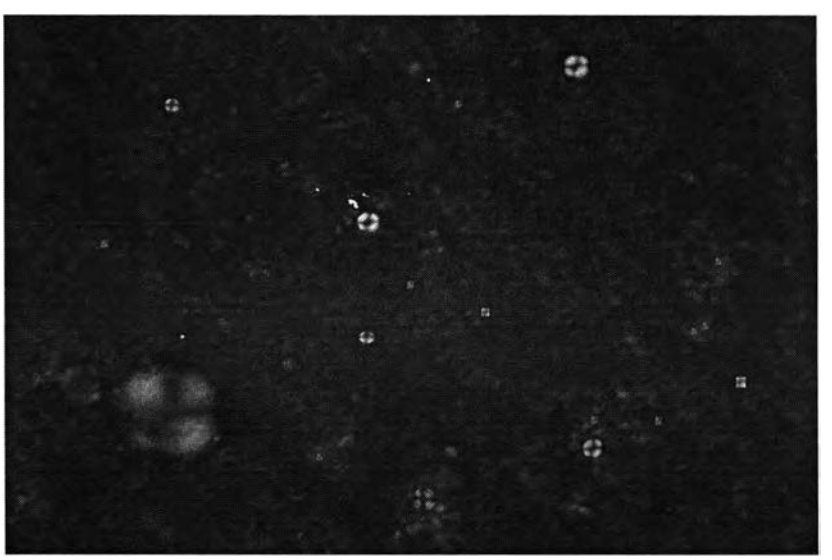

(d)

Figure 16. Polarized-light microscopic images of the vesicles from (a) Span® 40, (b) Span® 60, (C) Brij® 52, and (d) Brij® 76

3. Physical stability of MN niosomes

To estimate physical stability of niosomal preparations, MN niosomes contained in glass tubes wrapped in aluminum foil and tightly sealed with cap closures and paraffin films were stored at ambient conditions for three months. The influence of formulation factors on physical properties of niosomes, including the ability of niosomes to retain the entrapped MN was determined. The percentage of entrapment efficiency of MN in niosomes was analyzed by UV spectrophotometric method at 0, 1, 2, and 3 months, respectively.

By visual inspection, the color changes, and phase separation of all formulations were not evident during the period of three months. There was no gross precipitation of all niosomal formulations when inspected under an optical microscope. No drug crystal was found in any of the niosomal suspensions during three months of storage.

The entrapment efficiency of MN niosomes was determined at each time interval as shown in Table 7. Analysis of data indicates that the entrapment efficiency of all niosomal formulations at 0, 1, 2, and 3 months were not statistically different with respect to storage time ($p > 0.05$), using one-way analysis of variance followed by Tukey's HSD test. This implies that there was no severe destruction in niosomal structure during the storage intervals.

Table 7. The entrapment efficiencies of MN niosomes at 0, 1, 2, and 3 months of storage. The results are displayed as mean ± SD from three independent determinations.

Structural surfactant	Storage time (months)	MN in supernatant (mg)	Entrapped MN (mg)	Entrapment efficiency (μg/mg lipid)	% Entrapment	Total recovery
Span® 40	0	11.32 ± 0.06	1.91 ± 0.03	19.13 ± 0.26	86.94 ± 1.18	100.42 ± 0.67
	1	11.31 ± 0.03	1.91 ± 0.05	19.08 ± 0.52	86.73 ± 2.38	100.33 ± 0.65
	2	11.35 ± 0.11	1.90 ± 0.02	18.99 ± 0.21	86.33 ± 0.97	100.52 ± 0.96
	3	11.32 ± 0.12	1.92 ± 0.05	19.16 ± 0.51	87.08 ±2.30	100.40 ± 0.55
Span® 60	0	11.16 ± 0.20	2.10 ± 0.01	20.97 ± 0.05	95.32 ± 0.25	100.57 ± 1.53
	1	11.15 ± 0.31	2.09 ± 0.02	20.94 ± 0.24	95.17 ± 1.11	100.53 ± 2.51
	2	11.17 ± 0.19	2.10 ± 0.03	21.00 ± 0.293	95.46 ± 1.33	100.66 ± 1.36
	3	11.17 ± 0.35	2.09 ± 0.04	20.94 ± 0.40	95.17 ± 1.80	100.66 ± 2.60
Brij® 52	0	11.94 ± 0.07	1.43 ± 0.01	14.31 ± 0.12	65.06 ± 0.53	101.44 ± 0.58
	1	11.92 ± 0.18	1.43 ± 0.03	14.29 ± 0.35	64.97 ± 1.59	101.31 ± 1.59
	2	11.91 ± 0.07	1.42 ± 0.02	14.24 ± 0.21	64.75 ± 0.94	101.19 ± 0.53
	3	11.94 ± 0.05	1.42 ± 0.02	14.20 ± 0.25	64.56 ± 1.13	101.37 ± 0.50
Brij® 76	0	11.50 ± 0.23	1.70 ± 0.03	17.03 ± 0.35	77.43 ± 1.58	100.22 ± 1.64
	1	11.50 ± 0.34	1.71 ± 0.03	17.08 ± 0.29	77.65 ± 1.31	100.26 ± 2.42
	2	11.50 ± 0.23	1.69 ± 0.06	16.94 ± 0.56	77.00 ± 2.57	100.08 ± 1.36
	3	11.49 ± 0.32	1.71 ± 0.05	17.09 ± 0.45	77.69 ± 2.05	100.17 ± 2.11

4. Drug release studies

In vitro drug release is generally used in evaluation of drug delivery from topical formulations. The result from such experiment can predict the behavior of drug release to the skin in vivo (Wester and Maibach, 1990). In addition, the release data may be used to explain stability profiles of the drug expected to be protected from degradation by the dosage form.

The release profiles of MN from niosomal systems and from aqueous solution were plotted between the percentage of cumulative amounts of drug released and time as shown in Figure 17. The complete release data are presented in Appendix V. The rate of drug release through cellulose membrane from MN solution was faster than that from niosomal MN suspensions. The MN release profile from MN solution was linear over the first 6 h and then plateaued off. On the contrary, the release profiles from all vesicles were increasing over 24 h before reaching the plateau. The release profiles were relatively linear during the first 12 h, after which the release was much slower.

The results show that approximately 95% of the drug was released within 6 h. from the control solution, whereas the release of MN from niosomal preparations with Span® 40, Span® 60, Brij® 52, and Brij® 76 were about 68%, 55%, 77%, and 71%, respectively, during a period of 48 h. The release rate seemed to be related to the entrapment efficiency. The formulation with higher entrapment had a slower release rate. The Span® 60 formulation, which had the highest MN entrapment, yielded the slowest rate of release. This is in accordance with a previous study done by Guinedi et al. (2005), which compared Span® 40 and Span® 60 niosomes. It was likely that niosomes exhibited an alkyl chain length-dependent release as previously reported. Longer chain lengths usually result in lower release rates (Guinedi et al., 2005; Devaraj et al., 2002). These results are in agreement with earlier reports on control of drug release by niosomes (Ruckmani, Jayakar, and Ghosal, 2000; Guinedi et al., 2005; Alsarra et al., 2005). Rattanatraiphop (2000) attributed the slower propylthiouracil release from phospholipid liposomes to the fact that the drug did not diffuse freely, but the entrapped drug in the vesicles must diffuse through several barriers, including the membrane of adjacent vesicles. The same scenarios apply to niosomes as well. The release rates of other

substances (such as carboxyfluorescein, 5-fluorouracil, tretinoin, colchicine, and cytarabine hydrochloride) across the membrane from niosome preparations are lower than that of the free solution (Yoshioka, Sternberg, and Florence, 1994; Ruckmani, Jayakar, and Ghosal, 2000; Brisaert et al., 2001; Hao et al., 2002). The release rate of a drug from a dosage form is inversely related also to the vehicle viscosity. This consideration could partly account for different drug release profiles observed from vehicles with low viscosity such as the aqueous solution and those from vehicles with higher viscosity such as niosomal suspensions.

The results of this present study indicate that the diffusion through niosomal membrane was probably rate limiting. The differences observed in MN release among the various systems could be due to different thermodynamic activities of the drug in the vesicular formulations because the same drug concentration was used in all preparations. However, differences found in the release experiments could also be attributed to differences in niosomal compositions, resulting in different barrier properties, as well as differences in the size and shape of the vesicles. Devaraj et al. (2002) reported that the bilayer composition was a factor that dictated drug release from vesicles. The comparative release data in this present study indicate that, by niosome encapsulation, it was possible to sustain and control the release of the drug for a longer duration. However, under the actual conditions of topical use, the release from these vesicles may be modified due to the complicated processes involved, including vehicle evaporation and deformation of niosomal structure on the skin (Barry, 2001). Therefore, although the in vitro release of drugs from niosomes is very low, it is usually not a problem for topical use (Brisaert et al., 2001).

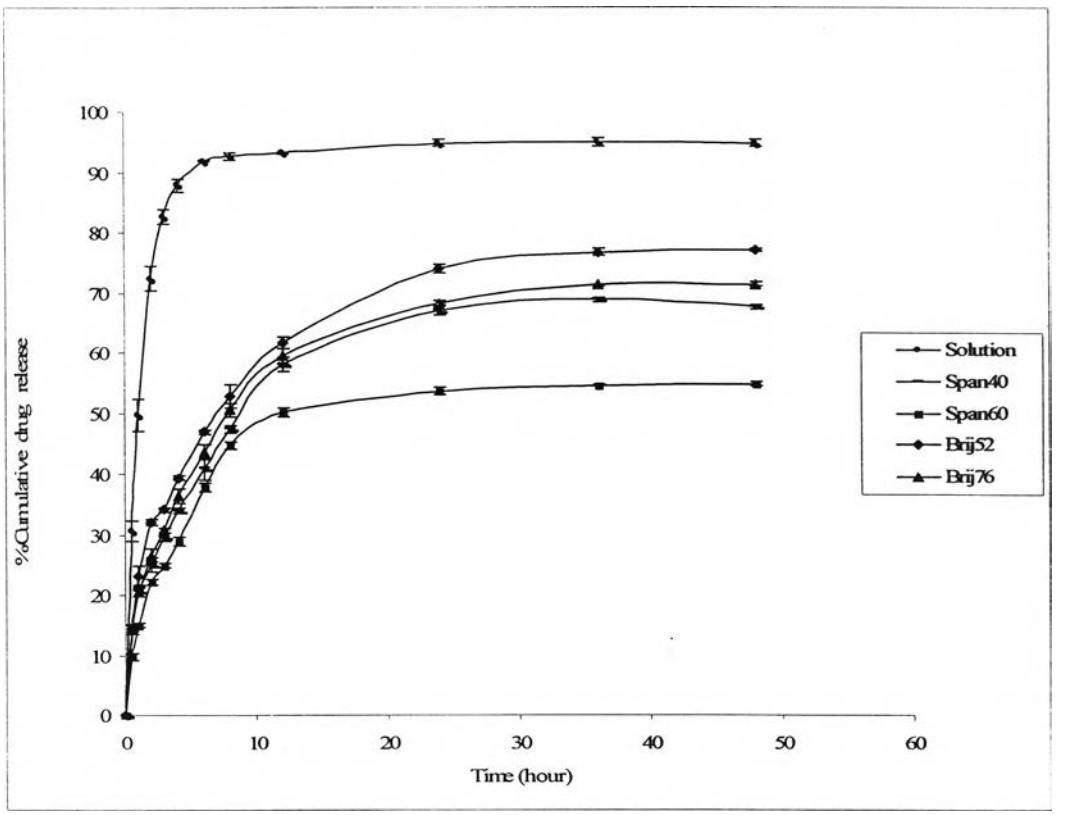

Figure 17. Release profiles of MN niosomes and aqueous solution. Data are displayed as mean ± SD, n = 3.

5. Chemical stability of MN niosomes

Chemical stability of MN niosomes at ambient temperature was studied for three months. The samples were wrapped with aluminum foil to protect the drug from UV light in a UV cabinet. The control was an aqueous solution of MN in water stored under the same conditions. The samples were also kept in the UV cabinet because this set of samples also served as the control in the next section to study the ability of niosomal vesicles to protect the drug from photodegradation. The amounts of MN in niosomes and solution were monitored by HPLC at 0, 10, 20, 30, 40, 50, 60, 70, 80, and 90 days.

The percentages of drug remaining of MN solution, Span® 40, Span® 60, Brij® 52, and Brij® 76 niosomes are shown in Table 8. MN contents were determined in both the

supernatants and the pellets for all niosomal formulations after centrifugation. The total recovery was higher than 99% in all cases. The entrapment efficiency and the amount of drug remaining in the preparations of MN niosomes were examined at each time interval and are displayed in Tables 9-12. No significant difference ($p > 0.05$) in the amounts of MN remaining in all preparations was observed at any time point when compared to T_0 by one-way analysis of variance followed by either Dunnett or Dunnett's T3 test. These results indicate that MN was stable over the three-month period in the absence of light both in the solution and in niosomal preparations at ambient temperature. The results of this study comply with those of Hainess-Nutt, Adams, and Bendell (1984) that MN solutions developed a slight yellow coloration after three months at room temperature, but no chemical degradation was seen after 6 months. Another stability study on MN was done by Pithayanukul (1988). Hydroalcoholic solution and hydroalcoholic gel of topical MN were formulated and investigated for the color change at room temperature (30 °C) with naked eyes. The results of that study showed that MN preparations containing propylene glycol turned into pink color, which resulted from the oxidation reaction between MN and propylene glycol. The author suggested that oxidation reaction was catalyzed by heavy metal impurities in propylene glycol and MN themselves. However, a chelating agent, 0.01% EDTA sodium, and an antioxidant, sodium bisulfite at a concentration of more than 0.5%, could inhibit the reaction.

However, Tuntiruttanasoontorn (1995) reported that degradation rate constants (k) at room temperature and at 70 °C of MN solutions were negligible. Nevertheless, the color of solutions kept at 70 °C turned into yellow after 2 weeks regardless of whether the solutions contained β-cyclodextrin (β-CD) and hydroxypropyl-β-cyclodextrin (HP-β-CD) or not. Thus, the additives such as β-CD and HP-β-CD could not prevent the color change of MN solution at 70 °C. In this study, MN did not undergo any chemical degradation after three months. The result was consistent with the previous studies (Haines-Nutt, Adams, and Bendell, 1984; Tuntiruttanasoontorn, 1995). Figure 18 displays a representation of HPLC chromatograms at the beginning and after three months of storage. The concentrations of MN did not differ significantly (Tables 9-12, $p > 0.05$) and no extra peaks were observed at three months, indicating that significant degradation did not occur over the period of study.

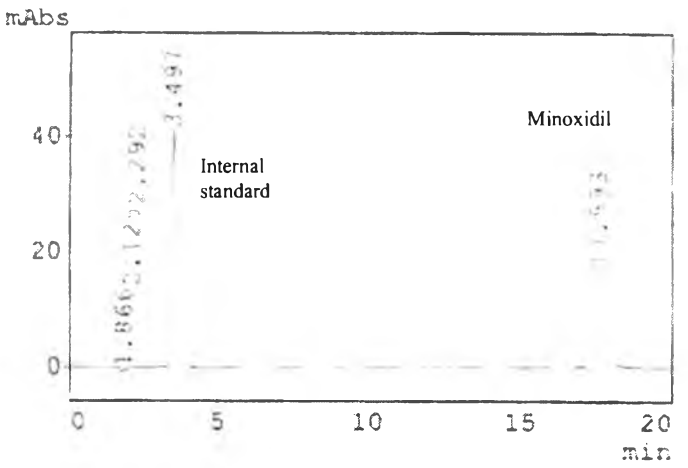

(a)

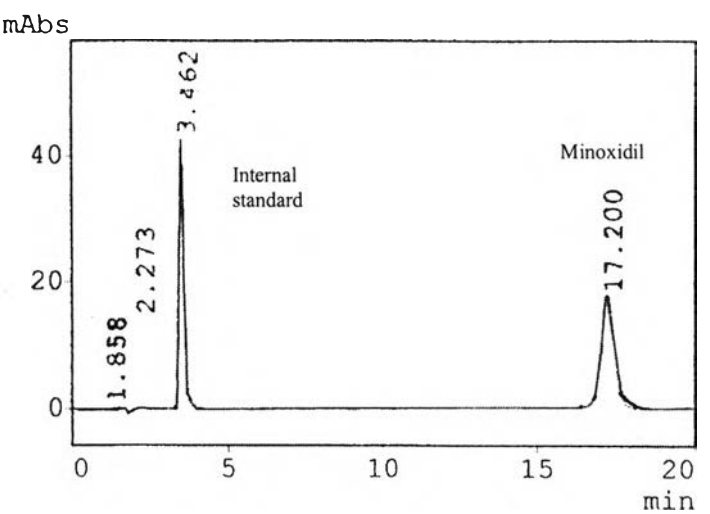

(b)

Figure 18. HPLC chromatograms at (a) the beginning and (b) after three months of storage

Table 8. The percentage of drug remaining of MN solution, Span® 40 niosomes, Span® 60 niosomes, Brij® 52 niosomes, and Brij® 76 niosomes during 3 months of storage. The results are displayed as mean ± SD from three independent determinations.

Storage time (days)	% Drug remaining				
	Solution	Span® 40 niosomes	Span® 60 niosomes	Brij® 52 niosomes	Brij® 76 niosomes
0	100.00 ± 0.00	100.00 ± 0.00	100.00 ± 0.00	100.00 ± 0.00	100.0000 ± 0.00
10	101.18 ± 1.57	99.81 ± 1.80	100.01 ± 0.81	99.60 ± 1.25	99.3278 ± 1.68
20	101.75 ± 2.03	98.45 ± 2.46	99.87 ± 1.10	100.07 ± 1.19	101.1791 ± 0.72
30	100.55 ± 3.45	99.24 ± 1.82	99.97 ± 0.28	100.23 ± 1.03	101.5593 ± 0.78
40	101.13 ± 2.26	99.26 ± 1.26	100.73 ± 0.22	100.49 ± 1.55	98.6564 ± 1.34
50	101.26 ± 0.44	100.35 ± 0.79	100.21 ± 1.36	100.75 ± 0.67	99.9615 ± 1.46
60	102.94 ± 0.65	100.34 ± 0.98	99.79 ± 0.13	99.91 ± 0.32	98.8660 ± 1.08
70	99.31 ± 0.08	99.53 ± 1.07	100.35 ± 0.24	100.42 ± 1.02	100.2952 ± 1.19
80	98.41 ± 1.03	98.78 ± 1.49	100.60 ± 0.33	100.67 ± 0.33	99.9600 ± 1.06
90	100.42 ± 2.10	98.91 ± 2.03	99.52 ± 0.27	100.74 ± 1.21	99.5003 ± 0.75

Table 9. The amounts of drug remaining in the supernatant and in the pellet, entrapment efficiency, and total recovery of MN niosomes prepared from Span® 40:Cholesterol:Solulan® C24 (67.5:27.5:5). The results are displayed as mean ± SD from three independent determinations.

Storage time (days)	MN in supernatant (μg)	Entrapped MN (μg)	Entrapment efficiency (μg/mg lipid)	Total recovery
0	11275.15 ± 31.88	1911.67 ± 2.06	19.12 ± 0.02	100.07 ± 0.25
10	11265.44 ± 16.08	1916.83 ± 1.71	19.17 ± 0.02	100.03 ± 0.11
20	11251.36 ± 21.34	1900.85 ± 3.40	19.01 ± 0.03	99.08 ± 0.17
30	11255.92 ± 9.69	1913.84 ± 11.55	19.14 ± 0.12	99.94 ± 0.07
40	11264.06 ± 11.21	1906.10 ± 6.00	19.06 ± 0.06	99.94 ± 0.04
50	11277.56 ± 21.31	1916.85 ± 2.57	19.17 ± 0.03	100.12 ± 0.17
60	11277.68 ± 13.83	1916.46 ± 5.35	19.17 ± 0.05	100.12 ± 0.09
70	11271.23 ± 9.61	1905.19 ± 2.47	19.05 ± 0.03	99.99 ± 0.07
80	11249.67 ± 27.25	1910.09 ± 6.79	19.10 ± 0.07	99.89 ± 0.22
90	11252.45 ± 14.78	1909.84 ± 2.32	19.10 ± 0.02	99.88 ± 0.11

Table 10. The amounts of drug remaining in the supernatant and in the pellet, entrapment efficiency, and total recovery of MN niosomes prepared from Span® 60:Cholesterol:Solulan® C24 (57.5:37.5:5). The results are displayed as mean ± SD from three independent determinations.

Storage time (days)	MN in supernatant (μg)	Entrapped MN (μg)	Entrapment efficiency (μg/mg lipid)	Total recovery
0	11159.62 ± 8.78	2032.80 ± 6.64	20.33 ± 0.07	100.11 ± 0.08
10	11160.43 ± 11.99	2032.23 ± 7.56	20.32 ± 0.08	100.11 ± 0.07
20	11160.65 ± 18.32	2028.94 ± 9.51	20.29 ± 0.10	100.09 ± 0.13
30	11150.78 ± 9.76	2040.95 ± 2.04	20.41 ± 0.02	100.10 ± 0.07
40	11168.11 ± 5.73	2040.38 ± 1.16	20.40 ± 0.01	100.23 ± 0.05
50	11166.89 ± 13.25	2030.16 ± 8.75	20.30 ± 0.09	100.14 ± 0.15
60	11151.71 ± 11.34	2036.01 ± 5.40	20.36 ± 0.05	100.07 ± 0.06
70	11172.16 ± 0.56	2027.98 ± 6.40	20.28 ± 0.06	100.17 ± 0.05
80	11172.74 ± 14.14	2032.91 ± 10.63	20.33 ± 0.11	100.21 ± 0.10
90	11154.90 ± 2.46	2026.91 ± 4.72	20.27 ± 0.05	100.03 ± 0.05

Table 11. The amounts of drug remaining in the supernatant and in the pellet, entrapment efficiency, and total recovery of MN niosomes prepared from by Brij® 52:Cholesterol:Solulan® C24 (67.5:27.5:5). The results are displayed as mean ± SD from three independent determinations.

Storage time (days)	MN in supernatant (μg)	Entrapped MN (μg)	Entrapment efficiency (μg/mg lipid)	Total recovery
0	11899.76 ± 24.59	1424.25 ± 3.76	14.24 ± 0.04	101.11 ± 0.17
10	11893.33 ± 20.73	1421.15 ± 4.53	14.21 ± 0.05	101.04 ± 0.15
20	11902.85 ± 15.75	1422.60 ± 2.51	14.23 ± 0.03	101.12 ± 0.13
30	11906.61 ± 8.25	1422.65 ± 2.59	14.23 ± 0.03	101.15 ± 0.06
40	11909.07 ± 15.65	1426.30 ± 3.32	14.26 ± 0.03	101.19 ± 0.12
50	11909.56 ± 14.89	1431.94 ± 4.85	14.32 ± 0.05	101.24 ± 0.11
60	11894.29 ± 11.79	1427.59 ± 5.58	14.28 ± 0.07	101.09 ± 0.13
70	11909.98 ± 16.06	1423.70 ± 4.02	14.24 ± 0.04	101.18 ± 0.14
80	11915.01 ± 15.22	1424.77 ± 5.77	14.25 ± 0.06	101.23 ± 0.15
90	11909.05 ± 5.39	1432.08 ± 7.91	14.32 ± 0.08	101.24 ± 0.10

Table 12. The amounts of drug remaining in the supernatant and in the pellet, entrapment efficiency, and total recovery of MN niosomes prepared from Brij® 76:Cholesterol:Solulan® C24 (47.5:47.5:5). The results are displayed as mean ± SD from three independent determinations.

Storage time (days)	MN in supernatant (μg)	Entrapped MN (μg)	Entrapment efficiency (μg/mg lipid)	Total recovery
0	11512.05 ± 27.89	1691.09 ± 9.18	16.91 ± 0.09	100.19 ± 0.14
10	11499.99 ± 19.02	1688.02 ± 3.74	16.88 ± 0.04	100.08 ± 0.16
20	11539.26 ± 4.80	1689.98 ± 4.37	16.90 ± 0.04	100.39 ± 0.06
30	11543.02 ± 8.67	1694.66 ± 5.69	16.95 ± 0.06	100.45 ± 0.04
40	11485.69 ± 16.27	1687.46 ± 2.25	16.88 ± 0.02	99.96 ± 0.13
50	11516.64 ± 15.71	1685.46 ± 6.74	16.86 ± 0.07	100.18 ± 0.11
60	11500.36 ± 5.20	1677.47 ± 7.23	16.78 ± 0.07	100.00 ± 0.09
70	11525.03 ± 6.90	1684.52 ± 7.52	16.85 ± 0.08	100.24 ± 0.09
80	11514.60 ± 7.82	1687.52 ± 4.09	16.88 ± 0.04	100.18 ± 0.04
90	11520.20 ± 11.45	1671.76 ± 7.52	16.72 ± 0.08	100.11 ± 0.06

6. Photodegradation study under UV irradiation

The photodegradation study was carried out by HPLC measurements performed on MN niosomes and MN solution just before exposure to UV radiation and at increasing times (0, 10, 20, 30, 40, 50, 60, 70, 80, and 90 days). Figure 19 shows a representation of HPLC chromatograms of MN solution before (T_0) and at 15 days of UV exposure. The chromatograms reveal several minor peaks of MN degradation products between 3.4 and 17.1 min, which were the results from photodegradation of MN in water. These minor peaks were not seen when MN preparations were protected from UV light by wrapping the containers with aluminum foil (Figure 18).

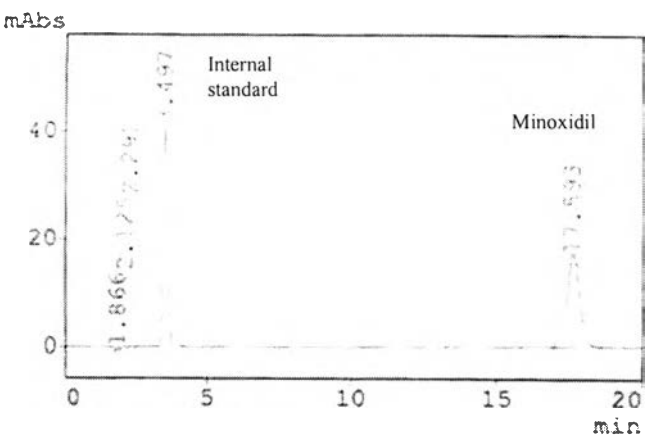

(a)

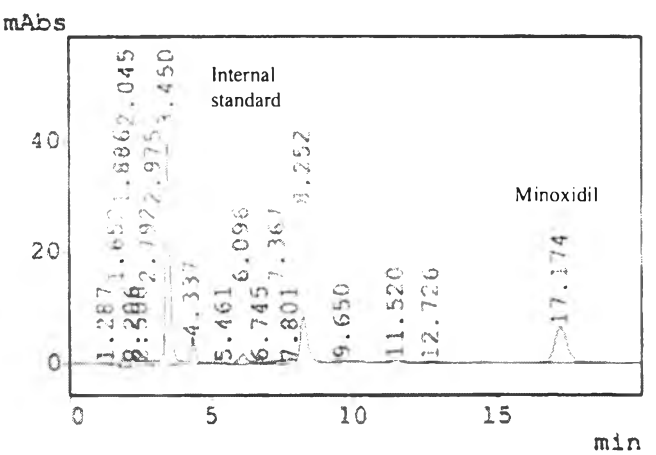

(b)

Figure 19. The HPLC chromatograms from photodegradation of MN in water: (a) before UV exposure and (b) after UV exposure

In this study, MN followed the first order kinetics and a good linearity was obtained by semi-log plot of percentage of drug remaining as a function of time. The result is in good agreement with a previous report by Chinnian and Asker (1996). The degradation of MN could be described by the following equation:

$$\ln A_t = -k_1 t + InA_0 \qquad (7)$$

where A_0 and A_t are the amounts of MN initially and at time t, respectively. k_1 is the first order degradation rate constant (day^{-1}), and t is the time (day).

The photodegradation rate constant of MN in aqueous solution (starting at 2.2 mg/ml) after 360 h of UV irradiation from triplicate analyses is 6.7 x 10^{-3} hr^{-1}. The degradation profile is shown in Figure 20. The detailed data are displayed in Table 13. In a previous report, the photodegradation rate constant of 4.5 μg/ml MN solutions exposed to intense fluorescent light (4.7 w/m^2, 39 ± 0.2 °C, in water) for 97 h was 4.6 x 10^{-3} hr^{-1}, which also followed the first-order kinetics (Chinnian and Asker, 1996). In the same study the degradation of MN in solution (20 °C, pH 7.0 phosphaste buffer) also followed first order degradation kinetics but with a rate constant of 9.464 x 10^{-3} day^{-1}. Chinnian and Asker (1996) also reported that MN solution was found to be more stable in phosphaste buffer as compared to acetate buffer. Besides, MN was found to be most stable in a solvent system of water or 25% v/v PEG 300 and least stable in 25% v/v propylene glycol.

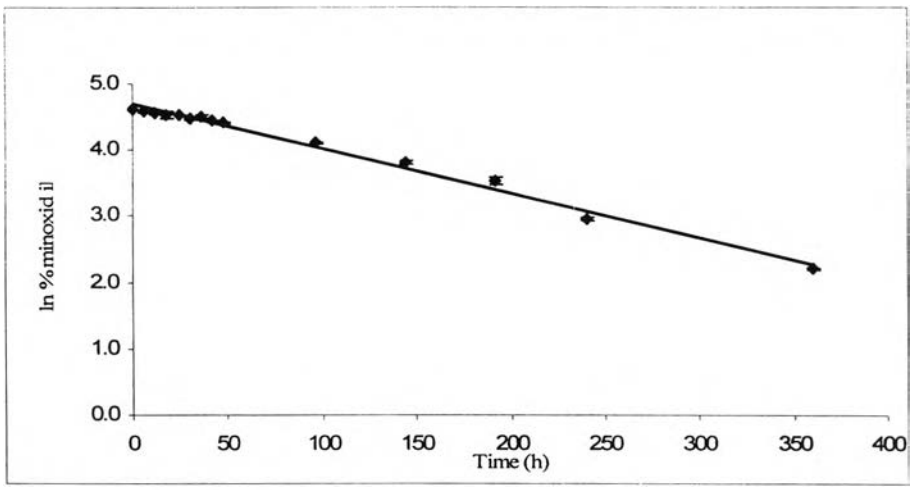

Figure 20. First-order degradation kinetics profile of MN in water. Data are presented as mean ± SD, n = 3.

Table 13. The percentages of drug remaining of MN solution exposed to UV light for 90 days. Data are shown as mean ± SD from three independent determinations.

Storage time (h)	% Drug remaining
0	100.00 ± 0.00
6	97.36 ± 0.75
12	94.67 ± 1.79
18	92.77 ± 4.19
24	92.14 ± 0.09
30	88.17 ± 2.37
36	89.63 ± 1.98
42	85.19 ± 0.93
48	81.99 ± 1.87
96	61.00 ± 0.92
144	44.97 ± 1.50
192	34.45 ± 2.24
240	19.32 ± 0.49
360	9.00 ± 0.17

Recent studies have demonstrated the positive action of niosomes as a carrier system for a number of photosensitive drugs (Habib and Asker, 1991; Loukas, Jayasekera, and Gregoriadis, 1995; Brisaert et al., 2001). The first goal of the present study was to investigate the potential of niosomes in stabilization of photodegradable MN under the conditions of accelerated UV irradiation. For photochemical reactions, UV light is the most potentially harmful radiation. The results in Figure 21 and Table 14 show that the percentages of remaining MN at day 90 were 84.97%, 70.54%, 68.16%, 57.78, and 9.00% for niosomal preparations composed of Span® 60, Span® 40, Brij® 76, Brij® 52 niosomes, and MN solution, respectively. Thus, niosomal preparations could efficiently stabilize MN from photodegradation under the conditions studied. MN in niosomes degraded much more slowly than that in solution.

However, the results also show that different niosomal preparations could stabilize MN to different degrees. Further analysis of data suggests that the differences seen among the niosomal preparations might result from the differences in the portion of unentrapped MN in these preparations. The ability of niosomal preparations in protecting MN from photodegradation could be ranked as follows: Niosomes consisting of Span® 60 > Span® 40 > Brij® 76 > Brij® 52. This ranking is in consistent with the release profiles of these preparations (see Figures 17 and 21). Niosomes prepared from Span® 60 had the slowest release rate. Thus, most of MN was retained in the niosomal vesicles, thus giving the drug best protection from the UV light. On the other hand, niosomes prepared from Brij® 52 released more MN, which allowed more exposure of the drug to UV radiation. Thus, more degradation resulted.

The overall data strongly suggest that MN in these preparations decomposed by photodegradation and that the niosomal structure could stabilize the drug. When kept in the absence of UV light, MN in both the supernatant and the pellet remained the same over the period of 90 days. The percentages of drug remaining of MN solution, Span® 40 niosomes, Span® 60 niosomes, Brij® 52 niosomes, and Brij® 76 niosomes are shown in Table 14. On the contrary, the amounts of MN in Span® 40, Span® 60, Brij® 52, and Brij®76 niosomal suspensions are statistically different ($p < 0.05$) from those at time 0 after only 10 days of exposure to UV radiation by one-way analysis of variance followed by Dunnett's test for all formulations (Table 15). In the presence of UV radiation,

amounts of MN in both the pellet and the supernatant decreased with time (Tables 16 and 17). The decrease of MN in the supernatant, however, tended to be more rapid than that in the pellet. The amounts of MN in the supernatant rapidly decreased, and significant deviations from Time 0 was seen after only 10 days of UV exposure for all formulations (Table 17). The amounts of MN in the pellet showed significant deviations from those at Time 0 after 60, 70, 20, and 40 days of UV exposure for Span® 40, Span® 60, Brij® 52, and Brij® 76, respectively (Table 16). The slower decrease of MN from the pellet was consistent with the slow release of the drug from the vesicles (Table 16 and Figure 17).

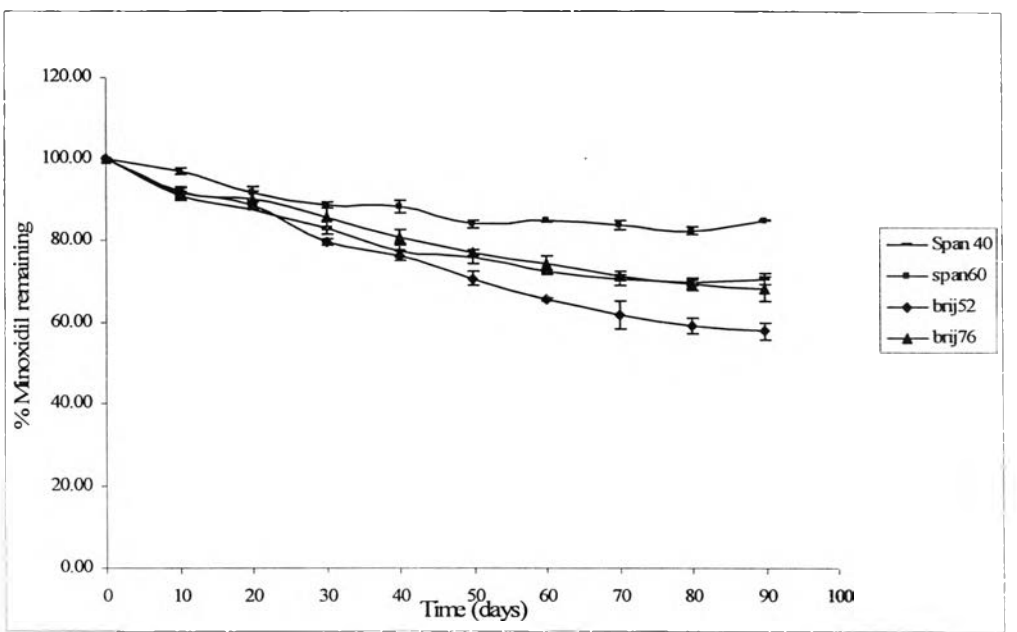

Figure 21. Photodegradation profiles of MN in niosomal suspensions under UV irradiation. Data are shown as mean ± SD from three independent determinations.

Table 14. The percentages of MN remaining in Span® 40, Span® 60, Brij® 52, and Brij® 76 niosomal suspensions exposed to UV light for 90 days. Data are shown as mean ± SD from three independent determinations.

Storage time (days)	% Drug remaining			
	Span® 40 niosomes	Span® 60 niosomes	Brij® 52 niosomes	Brij® 76 niosomes
0	100.00 ± 0.00	100.00 ± 0.00	100.00 ± 0.00	100.00 ± 0.00
10	90.94 ± 1.11	96.79 ± 0.68	92.02 ± 0.68	91.68 ± 1.45
20	87.55 ± 0.09	91.54 ± 1.73	88.40 ± 0.81	89.99 ± 2.17
30	83.02 ± 1.72	88.59 ± 0.79	79.65 ± 0.74	85.69 ± 3.04
40	77.39 ± 1.58	88.11 ± 1.43	76.13 ± 1.22	80.79 ± 1.87
50	75.75 ± 1.69	83.93 ± 0.89	70.48 ± 1.70	76.81 ± 0.81
60	72.18 ± 0.53	84.74 ± 0.21	65.62 ± 0.33	74.09 ± 2.06
70	70.38 ± 1.32	83.59 ± 1.11	61.76 ± 3.36	71.13 ± 1.06
80	69.76 ± 0.09	82.29 ± 0.84	59.09 ± 1.94	69.16 ± 1.24
90	70.54 ± 1.21	84.97 ± 0.21	57.82 ± 2.07	68.16 ± 2.91

Table 15. The amounts of MN remaining in niosomal suspensions prepared from in Span® 40, Span® 60, Brij® 52, and Brij® 76 at various time intervals of UV exposure. Data are shown as mean ± SD from three independent determinations.

Storage time (days)	Amount of MN remaining in niosomal suspension (μg)							
	Span® 40	p-value	Span® 60	p-value	Brij® 52	p-value	Brij® 76	p-value
0	2204.82 ± 32.87	-	2210.42 ± 10.62	-	2342.01 ± 22.01	-	2221.14 ± 18.77	-
10	2004.82 ± 17.98	0.000	2139.57 ± 19.97	0.001	2155.06 ± 19.79	0.000	2036.22 ± 25.63	0.000
20	1930.25 ± 28.79	0.000	2023.39 ± 31.53	0.000	2070.19 ± 0.93	0.000	1998.59 ± 31.86	0.000
30	1830.01 ± 11.14	0.000	1958.13 ± 9.39	0.000	1865.36 ± 18.08	0.000	1902.85 ± 52.10	0.000
40	1705.95 ± 19.14	0.000	1947.60 ± 23.56	0.000	1782.80 ± 19.99	0.000	1794.31 ± 30.70	0.000
50	1669.86 ± 30.89	0.000	1855.12 ± 19.47	0.000	1650.48 ± 34.71	0.000	1706.13 ± 28.29	0.000
60	1591.40 ± 13.11	0.000	1873.07 ± 11.68	0.000	1536.81 ± 7.66	0.000	1645.31 ± 33.24	0.000
70	1551.45 ± 8.23	0.000	1847.54 ± 16.02	0.000	1446.04 ± 65.65	0.000	1579.74 ± 11.01	0.000
80	1538.05 ± 17.06	0.000	1818.96 ± 10.52	0.000	1383.65 ± 38.81	0.000	1536.26 ± 33.44	0.000
90	1555.05 ± 5.12	0.000	1878.28 ± 4.70	0.000	1353.80 ± 39.09	0.000	1513.62 ± 55.85	0.000

Table 16. The amounts of MN remaining in niosomal pellets prepared from in Span® 40, Span® 60, Brij® 52, and Brij® 76 at various time intervals of UV exposure. Data are shown as mean ± SD from three independent determinations.

Storage time (days)	Amount of MN remaining in niosomal pellets (μg)							
	Span® 40	p-value	Span® 60	p-value	Brij® 52	p-value	Brij® 76	p-value
0	1911.67 ± 2.06	-	2032.80 ± 6.64	-	1424.25 ± 3.76	-	1691.09 ± 9.18	-
10	1919.19 ± 6.22	0.135	2020.74 ± 6.31	0.337	1426.88 ± 3.45	0.950	1686.12 ± 11.74	1.000
20	1909.19 ± 5.89	0.966	2027.04 ± 10.84	0.935	1414.48 ± 3.91	0.027	1683.01 ± 5.72	0.986
30	1914.56 ± 1.38	0.926	2035.29 ± 7.41	1.000	1409.62 ± 4.85	0.001	1658.87 ± 21.42	0.073
40	1907.59 ± 2.00	0.707	2045.16 ± 6.92	0.314	1411.26 ± 2.02	0.003	1623.82 ± 16.63	0.000
50	1904.67 ± 1.69	0.183	2016.45 ± 12.19	0.103	1397.79 ± 3.36	0.000	1608.76 ± 3.09	0.000
60	1898.29 ± 4.16	0.002	2046.18 ± 4.84	0.241	1396.02 ± 3.61	0.000	1620.14 ± 23.23	0.000
70	1895.64 ± 4.87	0.000	2007.32 ± 5.74	0.005	1400.05 ± 5.38	0.000	1591.76 ± 21.68	0.000
80	1894.69 ± 3.07	0.000	2005.50 ± 8.86	0.002	1390.70 ± 0.99	0.000	1563.37 ± 1.54	0.000
90	1893.52 ± 2.30	0.000	2000.18 ± 3.53	0.000	1394.07 ± 3.75	0.000	1572.99 ± 5.67	0.000

Table 17. The amounts of MN remaining in the supernatant prepared from in Span® 40, Span® 60, Brij® 52, and Brij® 76 at various time intervals of UV exposure. Data are shown as mean ± SD from three independent determinations.

Storage time (days)	Amount of MN remaining in the supernatant (μg)							
	Span® 40	p-value	Span® 60	p-value	Brij® 52	p-value	Brij® 76	p-value
0	11275.15±31.88	-	11159.62±8.78	-	11899.76±24.59	-	11512.05±27.89	-
10	11067.63±14.14	0.000	11100.83±13.97	0.000	11710.19±17.61	0.000	11332.10±23.14	0.000
20	11003.06±23.45	0.000	10978.35±22.12	0.000	11637.72±4.45	0.000	11297.58±28.53	0.000
30	10897.46±10.60	0.000	10904.84±6.89	0.000	11437.74±17.59	0.000	11225.98±43.35	0.000
40	10780.36±19.70	0.000	10884.45±19.51	0.000	11353.54±21.42	0.000	11152.49±14.20	0.000
50	10747.18±29.44	0.000	10820.67±14.87	0.000	11234.69±38.06	0.000	11079.37±26.15	0.000
60	10675.11±13.32	0.000	10808.89±11.16	0.000	11122.79±4.05	0.000	11007.16±10.34	0.000
70	10637.82±4.12	0.000	10822.22±10.32	0.000	11027.99±68.66	0.000	10969.98±18.12	0.000
80	10625.35±15.07	0.000	10795.46±2.92	0.000	10974.95±39.71	0.000	10954.90±34.96	0.000
90	10643.53±6.95	0.000	10860.10±7.77	0.000	10941.72±42.83	0.000	10922.63±51.34	0.000

Several authors reported that drug stability may be improved by its incorporation in vesicular bilayers. The stability of the photosensitive drug in vesicular suspensions is affected by the properties of the vesicles themselves. Therefore, the composition and structure of vesicles should be considered in liposomal and niosomal formulations of photosensitive drugs (Manconi et al., 2003; Ioele et al., 2005; Bandak et al., 1999; Habib and Asker, 1991; Pallozza et al. 2006). In previous study, Manconi et al. (2003) compared the chemical stability of tretinoin in methanol and in vesicular suspensions exposed to UV irradiation. After UV irradiation, tretinoin dissolved in methanol degraded very quickly while incorporation of the drug in vesicles always led to a reduction in photodegradation. The photoprotection offered by vesicles varied depending on the vesicle structure and composition. Brisaert et al. (2001) investigated the chemical stability of tretinoin with xenon lamp. They found that vesicle preparations also degraded in the presence of light but were more stable than when tretinoin was dissolved in castor oil that seemed to be the best solvent for photostability of tretinoin in their study. A possible explanation for this finding is that the incorporated drug is less accessible to light beams because of light scattering by the vesicles.

Loukas, Jayasekera, and Gregoriadis (1995) found that photodegradation of a photosensitive drug (riboflavin) in water placed in front of a UV light (6W and 460 $\mu Wcm^{-2}dm^{-1}$) was faster than that of vesicular formulations. The formulations tested included riboflavin multilamellar vesicles and riboflavin containing vesicles that were prepared in the absence of lipid- and water-soluble UV absorbers. However, vesicles containing the γ-cyclodextrin inclusion complex of the vitamin within the aqueous phase and the light absorbers (oil red O, oxybenzone, and dioxybenzone) together with the antioxidant β-carotene in the lipid phase provided the optimal protection of riboflavin. Habib and Asker (1991) reported that neutral and negatively charged liposomes increased photostability of riboflavin under fluorescent light. On the contrary, positively charged liposomes decreased riboflavin photostability. Besides, enhanced photostabilization seemed to be higher in alkaline pH than in acidic pH. However, the ionic strength of solution appeared to demonstrate no significant effect.

The vesicular structure seems to be important in protecting the drug from photodegradation. The photodegradation of doxorubicin encapsulated in

polyethyleneglycol-coated liposomes under UV-A light was significantly lower in comparison to the photodegradation of the free drug and showed no concentration dependency (Bandak et al., 1999). During and after UV-A irradiation, there was no leakage of the drug from liposomes to the medium. After induced leakage of doxorubicin from the liposomes, the degradation kinetics of the drug was identical to that of free doxorubicin. The results of this present study seem to support these findings.

7. Estimation of the irritation potential of MN niosomes

This study employed the principle of red blood cell hemolysis to determine the potential of niosomal formulations in causing irritation. The mechanism of hemolysis by surfactants may be described in three steps. Firstly, the surfactant molecules bind to erythrocyte membrane by lipophilicity. Secondly, the molecules are further incorporated into the interior of lipid bilayer of cell membrane and result in disruption of bilayer structure as well as a change in cell shape and consequent small lesions. Thirdly, small solutes permeate through the lesions, which induce an osmotic change across the membrane. Thus, the degree of damage to red blood cell membrane would correlate with the adsorption of the nonionic surfactant to the erythrocytes (Kobayashi, Onukui and Tachibana, 1999).

SDS, a moderately irritating anionic surfactant, is used world wide as the standard irritant for biological research on the skin and bodily systems. The concentration of each preparation that caused 50% hemolysis (H_{50}) is usually compared to the standard irritant. The results of this present study are shown in Table 18. The complete data are also presented in Appendix VI. The data reveal that all preparations tested were less irritating than SDS. Among these, Brij® 76 as free surfactant molecules or micelles was the most possible to cause irritation with the H_{50} of 7.4% v/v. MN in the vehicle used in the commercial product was more irritating than MN in water and in niosomes. However, hemolysis potential of MN niosomes showed tendency to increase with an increase in hydrophobic chain length (Brij® 76 > Brij® 52). The results related to the hemolytic action observed in the present study are contrasting to those previously reported with new arginine-based surfactants in human erythrocytes (Benavides et al., 2004). The hemolytic

action of the arginine-based surfactants studied showed a clear tendency to decrease with increase in hydrophobic chain length. The most hemolytic of them all were the surfactants with shorter chains (8 and 10 carbon atoms). The dermal irritation predicted from the cytotoxic effect on 3T6 fibroblasts suggested that the arginine-based surfactants with 12 carbon atoms were less irritating. The maximum irritation of 8,8,-L-arginine and 10,10-L-arginine can be attributed to the combination of a number of physicochemical parameters: hydrophobicity, adsorption, critical micelle concentration, and aqueous solubility, with the solubility being the limited step for the transport across the membrane. However, interpretation of in vitro results is not always straightforward. Hofland et al. (1992) reported in vitro studies on a ciliotoxicity model to estimate the toxicity of alkyl polyoxyethylene niosomes on the nasal mucosa. The studies revealed that an increase in alkyl chain length was accompanied by a decrease in toxicity to nasal mucosa while an increase in the polyethylene chain length caused an increase in ciliotoxicity. In general an increase in chain length increases the gel to liquid phase transition while an increase in the length of the polyoxyethylene chain decreases the gel to liquid phase transition (Hofland et al., 1992). This study concluded that gel state niosomes were less ciliotoxic than the liquid state vesicles. It is worthwhile to note that the authors stated that the HLB number had no influence on the toxicity of the compounds; the more hydrophobic compounds were obviously less toxic.

Neither the length of the polyoxyethylene chain nor the alkyl chain had any influence on the skin toxicity of alkyl polyoxyethylene niosomes as assessed by the cell proliferation of human keratinocytes in vitro (Hofland et al., 1991, 1992). The nature of the linkage (ester or ether) is also a determining factor in this model, where the more labile ester bond is usually found to be more toxic than the ether bond (Uchegbu and Vyas, 1998). However, the contrary was found in this present study with MN niosomes. Span® surfactant, which has the ester linkage, was less toxic than Brij® surfactant, which has the ether linkage. Nevertheless, the irritation potential of all formulations with MN was similar to the corresponding systems without the drug. Thus, MN itself did not impose any irritation potential. The overall results indicate that MN niosomes did not show much potential to cause irritation to the mucous membrane.

Table 18. Concentrations of MN niosomes and other corresponding components that caused 50% hemolysis

Component	50% Hemolysis (%v/v)
Sodium dodecyl sulphate (1 mg/ml)	1.7
Span® 40 (67.5 mg/ml)	> 97.5
Span® 60 (57.5 mg/ml)	> 97.5
Brij® 52 (67.5 mg/ml)	64
Brij® 76 (47.5 mg/ml)	7.4
Cholesterol (47.5 mg/ml)	> 97.5
Solulan® C24 (5 mg/ml)	> 97.5
MN Span® 40 niosomes (100 mg total lipid/ml) *	81.5
MN Span® 60 niosomes (100 mg total lipid/ml)**	> 97.5
MN Brij® 52 niosomes (100 mg total lipid/ml)***	56.1
MN Brij® 76 niosomes (100 mg total lipid/ml)****	51.8
MN in water (2.2 mg/ml)	47.5
MN in vehicle in the commercial product (2.2 mg/ml)	17.6
Span® 40 niosomes (100 mg total lipid/ml) *	81.8
Span® 60 niosomes (100 mg total lipid/ml)**	> 97.5
Brij® 52 niosomes (100 mg total lipid/ml)***	55.9
Brij® 76 niosomes (100 mg total lipid/ml)****	52.1
Water	47.2
Vehicle in the commercial product	17.6

* ratio of Span® 40:CHO:Solulan® C24 = 67.5:27.5:5

** ratio of Span® 60:CHO:Solulan® C24 = 57.5:37.5:5

*** ratio of Brij® 52:CHO:Solulan® C24 = 67.5:27.5:5

**** ratio of Brij® 76:CHO:Solulan® C24 = 47.5:47.5:5